Solar impact on the lower mesospheric subtropical jet: A comparative study with general circulation model simulations

Kunihiko Kodera,[1] Katja Matthes,[2] Kiyotaka Shibata,[1] Ulrike Langematz,[2] and Yuhji Kuroda[1]

Received 19 August 2002; revised 24 December 2002; accepted 26 December 2002; published 26 March 2003.

[1] The seasonal and interannual variation in the lower mesospheric subtropical jet (LMSJ) and their dependence on the 11-year solar cycle are studied by comparing observational data with simulations by two general circulation models. In the model simulations, a strengthening of the LMSJs is found in both hemispheres during the winter under the solar maximum condition, similar to the observation. However the model responses are substantially smaller except for one case in the southern hemisphere. It is also found that the stronger LMSJ due to an enhanced solar forcing appears during the period which follows an increasing period of interannual variation. Analysis of the observed seasonal march of the LMSJ in each year shows two different regimes of behavior. For a successful simulation, the model should realistically reproduce the observed interannual variability as well as the climatological mean. *INDEX TERMS:* 3334 Meteorology and Atmospheric Dynamics: Middle atmosphere dynamics (0341, 0342); 3319 Meteorology and Atmospheric Dynamics: General circulation; 1650 Global Change: Solar variability. **Citation:** Kodera, K., K. Matthes, K. Shibata, U. Langematz, and Y. Kuroda, Solar impact on the lower mesospheric subtropical jet: A comparative study with general circulation model simulations, *Geophys. Res. Lett.*, *30*(6), 1315, doi:10.1029/2002GL016124, 2003.

1. Introduction

[2] A substantial dynamical response to solar cycle variations has been reported in the stratopause region during the winter: the zonal-mean zonal wind around the subtropics of the stratopause varies by more than 10 ms^{-1} between the solar maximum and minimum phases [*Kodera and Yamazaki*, 1990; *Hood et al.*, 1993]. Wind anomalies created in the subtropics of the stratopause region propagate poleward and downward [*Kodera*, 1995] and even affect the tropospheric circulation [*Shindell et al.*, 2001, *Kuroda and Kodera*, 2002]. Because the observational data are not long enough, and the model performance is far from perfect, it is important to identify the initial solar impact and understand the mechanism which produces the large impact.

[3] It should be noted that the zonal wind variation during a solar cycle simulated by a two-dimensional model is only about 0.5 ms^{-1} [*Huang and Brasseur*, 1993], i.e., more than one order of magnitude smaller than the observations. This suggests that the large impact in the winter stratosphere is produced through wave mean-flow interaction with planetary waves. In a recent observational study, it was suggested that the solar cycle influence can be seen as a modulation of the transition from a radiatively controlled state in early winter to a dynamically controlled one in late winter [*Kodera and Kuroda*, 2002].

[4] In the present paper, observational results are compared with two general circulation model (GCM) simulations to i) identify the mechanism of solar influence and ii) assess the model performance. Here, we focus on a specific issue of the large zonal wind response near the stratopause.

2. Data

[5] The observational data is the same as in *Kodera and Kuroda* [2002]. Balanced winds are calculated from the geopotential height data analyzed by the Climate Prediction Center/National Centers for Environmental Prediction [*Randel*, 1992]. According to solar 10.7 cm radio flux, maximum and minimum phases of the solar cycle are defined during the recent two solar cycles 1979–1998: for maximum phases, years 1979–1982 and 1988–1991, and for minimum phases, years 1984–1987 and 1994–1997 [see *Kodera and Kuroda*, 2002].

[6] The design of the GCM experiment is essentially the same as that conducted by *Haigh* [1999]. The solar energy spectrum change during a solar cycle from 120 to 420 nm is estimated by *Lean et al.* [1997], and the resultant ozone variation is calculated using the Imperial College two-dimensional chemical model [*Haigh*, 1994]. The same ozone change was introduced in the Meteorological Research Institute (MRI) and Freie Universität Berlin (FUB) GCMs and the heating rate change resulted from the change in irradiance and ozone. The MRI model has a horizontal resolution of T42 with 45 vertical layers from the surface to 0.01 hPa [*Shibata et al.*, 1999], and the FUB model has a horizontal resolution of T21 with 34 vertical layer up to 0.0068 hPa [*Langematz and Pawson*, 1997]. Both models are integrated for 20 years separately under solar maximum and solar minimum conditions and with prescribed seasonally varying climatological sea surface temperatures at the lower boundary.

3. Results

[7] Figure 1 shows the observed zonal-mean zonal wind differences between the maximum and minimum phases of the solar cycle during the winter solstice, (a) June in the southern hemisphere (SH) and (b) December in the northern hemisphere (NH). Enhanced zonal wind velocity during the solar maximum phases is observed in both hemispheres from the upper stratosphere to the lower mesosphere. Anomalous westerlies increase with altitude until the top

[1]Meteorological Research Institute, Tsukuba, Japan.
[2]Institut für Meteorologie, Freie Universität Berlin, Berlin, Germany.

0094-8276/03/2002GL016124

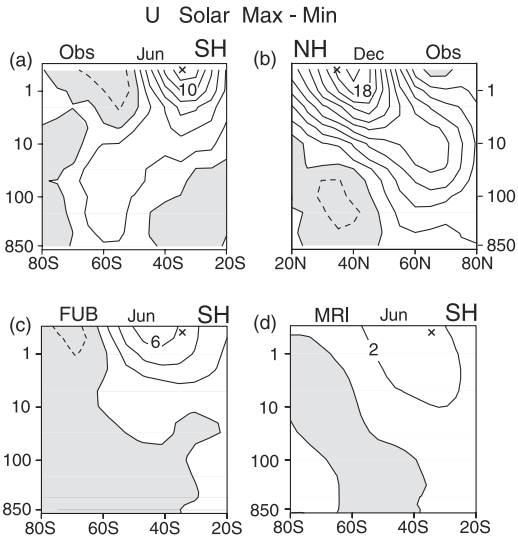

Figure 1. Zonal-mean zonal wind difference between the maximum and minimum phases of the 11-year solar cycle. Observed changes in (a) June in the SH, and (b) December in the NH. (c) and (d) are the same as in (a) but for a model simulation with FUB and MRI GCMs, respectively. Contour interval is 2 ms^{-1} and negative values are shaded. Symbol × denotes the location 0.4 hPa, 35° latitudes.

level of the observation (0.4 hPa). The results of model simulations in the SH by FUB and MRI are displayed in Figures 1c and 1d, respectively. Both models simulate a stronger subtropical jet during the solar maximum phase. The magnitudes of the simulated solar response is about 6 ms^{-1} in the FUB model, about a half of the observation, whereas in the MRI model it is about 3 ms^{-1}, a quarter of the observation. Model responses of the lower mesospheric subtropical jet (LMSJ) in the NH are even smaller and are not shown here.

[8] It should be noted that the thermal response in the equatorial stratopause region is quite similar in both models. Under solar maximum conditions, the shortwave heating rate increases by about 0.2 K/day in the equatorial stratopause, which produces 0.75–1.0 K higher temperatures in this region, comparable to observations. Therefore, the origin of the different solar response among the models should be searched for in the different dynamical properties of the models.

[9] To investigate in more detail we have selected the zonal-mean zonal wind at 35° latitude in the SH and NH at 0.4 hPa, which approximately corresponds to the core of the westerly anomalies in both hemispheres (Figure 1). For simplicity, the zonal-mean zonal wind at this location is hereafter denoted as the lower mesospheric subtropical jet (LMSJ). Time series of the mean difference in the LMSJ between the solar maximum and minimum phases are shown in Figure 2 with filled curves for (a) observation, (b) FUB, and (c) MRI model simulations. Top panels are for the SH from March through July, and bottom panels are for the NH from September through January. Stronger LMSJs are observed around the winter solstice in both hemispheres during the maximum phase of the solar cycle. Both models simulate an increase in the wind speed of the LMSJ but their amplitudes are smaller.

[10] In Figure 2, the standard deviation of LMSJ in each month from the climatology is also displayed by dashed lines for each of the solar maximum (open circles) and minimum (closed circles) phases. Here, a standard deviation indicates the amplitude of the interannual variability. It can be seen that the solar response is not necessarily maximum at the solstice, but a larger amplitude appears following a period of increasing standard deviation.

[11] Usually, the interannual variation is considered as a background noise to the solar signal, and the statistical significance is calculated based on this assumption. However, the above result suggests a highly non-linear nature of the solar signal response. To investigate in more detail the relationship between the interannual variation and the solar response, time series of the LMSJ are displayed in each year from autumn to winter in the SH (Figure 3) and NH (Figure 4) for (a) observations, (b) FUB, and (c) MRI model simulations. Top panels are for solar maximum condition, and bottom panels are for solar minimum condition. Observation and model simulations include eight and eighteen years, respectively.

[12] The distribution of wind speed of the observed LMSJs in the SH (Figure 3a) exhibits a clear difference between the maximum and minimum phases. During the solar maximum, LMSJs increase almost linearly from March until June. As a result, LMSJs have high speeds exceeding 80 ms^{-1} in June during solar maximum. In contrast, at solar minimum, the increasing speed of the LMSJ slows down from May and stays at low speeds for nearly half of the cases. Thus, at solar minimum, the LMSJs tend to be clustered around 90 ms^{-1} and around 70 ms^{-1} in June. To display the difference in the distribution of the wind speed between the solar maximum and minimum phases, the LMSJs are subjectively grouped in two types, high speed (solid lines) and low speed (dashed lines) one. At solar maximum, high speed type appears exclusively, whereas during solar minimum high- and low speed types occur equally.

[13] In the observations, the number of samples is small (eight years), but similar characteristic can also be found in

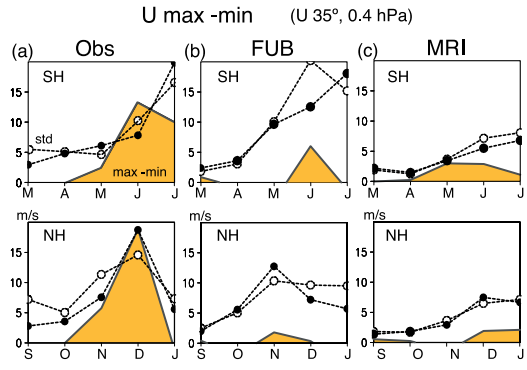

Figure 2. (Filled curve): Time series of the differences in the monthly mean zonal-mean zonal wind between the solar maximum and minimum phases at 0.4 hPa, 35° latitude, for (a) observations, (b) FUB, and (c) MRI simulations. Top and bottom panel panels are for the SH and NH winters, respectively. Dashed lines indicate standard deviation of the monthly mean LMSJ for minimum (open circles) and maximum (closed circles) phases, respectively.

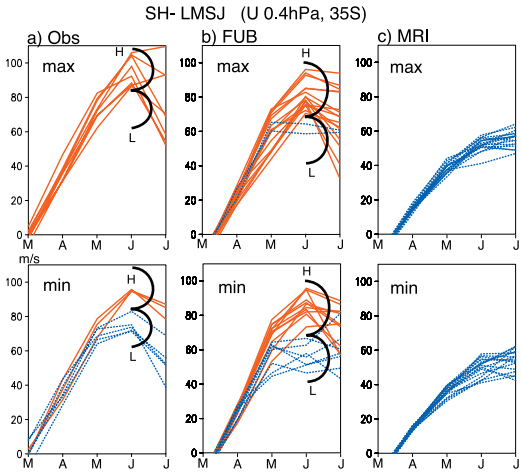

Figure 3. Time series of individual monthly mean zonal-mean zonal wind at 0.4 hPa, 35° S in SH cold season from March through July. (a) observations, (b) FUB, and (c) MRI simulations. Top and bottom panels are for the solar maximum and minimum cases, respectively. Solid and dashed lines denote two groups of high (H) and low (L) speed LMSJ, respectively (see text).

FUB simulation (Figure 3b). For solar maximum conditions, except for two winters, LMSJs steadily increase until June (solid lines), while for solar minimum conditions, the LMSJs stop increasing in May in seven of the winters (dashed lines). In the MRI simulation (Figure 3c), the increase of the LMSJs is gradual comparable to observations and the FUB simulation. LMSJs keep increasing until June. Although the difference is small, two different increasing tendencies, rapid and slower ones, can still be recognized during May–June. The slowly growing case is found four times during solar minimum but only once for solar maximum. It is also noted that the interannual variation in the MRI model is substantially smaller.

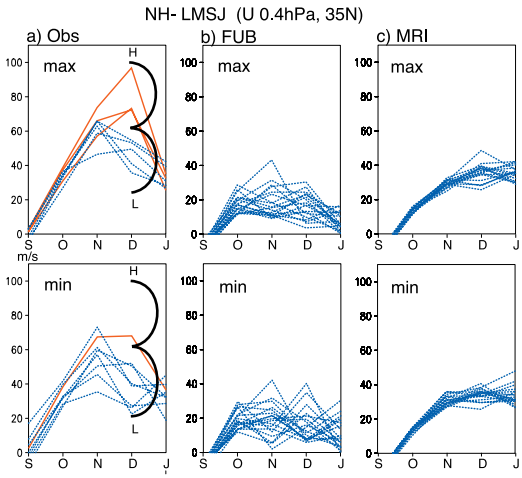

Figure 4. The same as in Figure 3, but for the zonal-mean zonal wind at 35°N in NH cold season from September through January.

[14] In the NH, at solar maximum, observed LMSJs can be divided into two groups (Figure 4a). The LMSJs in the first group continue to increase until December and reach higher speeds (>65 ms^{-1}) (solid lines), whereas in the second case, the LMSJs start to decrease from November and have lower speeds (<55 ms^{-1}) (dashed lines). During the solar minimum phases, all LMSJs sharply decrease from November except for one winter.

[15] In the FUB simulation of the NH (Figure 4b), LMSJs slow down prematurely in October in more than half of the cases and keep extremely low speeds under solar minimum conditions. The LMSJs increase until November slightly more often under the solar maximum condition. The LMSJs of the MRI simulation in the NH (Figure 4c) exhibit similar characteristics to those in the SH: a gradual increase and a small interannual variation. For solar maximum conditions, the LMSJ increases until December, except for four cases, whereas under solar minimum conditions, the LMSJ slow down more frequently in November.

4. Discussion and Concluding Remarks

[16] A large solar response is observed in three cases: in the SH and NH of the observations, and the SH of the FUB simulation (Figure 1). In these cases, regime-like structures with high (H) and low (L) LMSJ speeds can be recognized especially during the solar minimum phase in the SH and solar maximum phase in the NH. The large solar responses in Figure 1 are due to a change in the occurrence frequency of two groups during the different phases of the solar cycle.

[17] The relationship between the internal variation of the winter stratosphere and the response to the solar cycle forcing is schematically illustrated in Figure 5. According to the change in solar zenith angle, differential radiative heating rate increases from autumn to winter, and the LMSJ increases with time until the deceleration by the planetary waves propagating from the high latitude of the lower stratosphere becomes dominant. Wave forcing can differ from one year to another, so that the balance between the

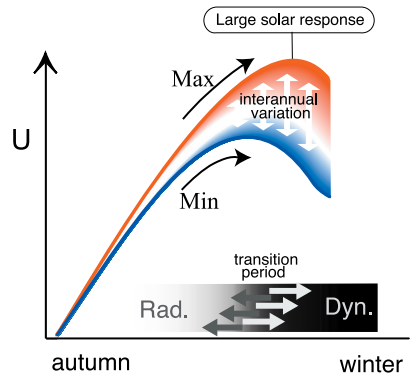

Figure 5. Schematic illustration of the relationship between the interannual variation of the winter atmosphere and the response to the solar cycle forcing. Large interannual variation occurs around the climatological transition period. Regime-like structure during this period produces large dynamical response to the solar forcing (see text).

radiative and dynamical forcing differs in each year. As discussed in *Kodera and Kuroda* [2002], the variation of the wave forcing is not necessarily due to the change in the wave source in the troposphere, but it can be produced in the stratosphere by change in the propagating condition. When the wave forcing is weaker, the LMSJ tends to develop until late winter, whereas when wave forcing is stronger, the LMSJ tends to decrease earlier. Accordingly, during the climatological transition period, a regime-like structure (high speed or low speed jet) appears in LMSJ distribution. This period is also characterized by large interannual variation. The atmospheric circulation appears to be particularly sensitive to the change in external forcing, i.e., solar forcing, during the period when the regime like structure develops. High speed LMSJs occur more frequently during solar maximum conditions and low speed ones occur more frequently during solar minimum conditions. The large amplitude of solar response is thus explained by a regime-like structure of the LMSJ and its sensitivity to the external forcings.

[18] The relationship between the period of increasing standard deviation and the peak period of the solar response may be explained by the above mechanism. The increase of the standard deviation implies the start of wave mean-flow interaction, which can create bi-modal structure in the distribution of zonal mean flow speeds. Thus, the period of increasing standard deviation corresponds to the development of the regime structure. At this stage, the atmospheric circulation should be particularly sensitive to the change in external forcing [*Palmer*, 1993]. Therefore, a large solar response is expected during this period.

[19] Only high speed LMSJ appears during the solar maximum phase in the SH. In contrast, the low speed LMSJ regime dominates during the minimum phases in the NH. A bi-modal structure appears at solar minimum in the SH but at solar maximum in the NH (Figures 4a and 5a). The solar forcing should be higher during the solar maximum phases than the minimum phase and the planetary wave forcings should be smaller in the SH than that in the NH. We suggest therefore that the right balance between the radiative and dynamical forcing is crucial for a bi-modal structure to be formed.

[20] In the observed LMSJ, the bifurcation between the high and low speed jet occurs around the wind speeds of 60–80 ms^{-1} (Figures 3a and 4a). The FUB model simulation in the SH, which has a comparable LMSJ wind speed (70 ms^{-1}) also shows a regime-like structure. However, the LMSJs in other simulations are very weak (<60 ms^{-1}) and regime-like structure is not apparent. Smaller solar responses in the model simulations, in particular, in the NH can be understood by a failure to reproduce realistic speeds of the LMSJs.

[21] So for a better model simulation, the improvement of the jet profile should be crucial. The bad performance of the present model simulations may be due to the Rayleigh friction used in FUB- and MRI-GCMs as a crude parameterization of gravity wave forcings. However, the problem of a weak subtropical jet (and strong polar night jet), is a common problem of GCMs [*Pawson et al.*, 2000]. Another problem seen in the MRI model is the smallness of the internal variability. The amplitude of the solar response is related to the magnitude of the regime-like structure, i.e., that of interannual variability. It is, therefore, important not only to reproduce the climatological feature but also to realistically simulate the interannual variation in the model.

[22] **Acknowledgments.** The authors thank J. Lean and J. Haigh for providing solar energy spectrum and ozone variation data. This study is conducted as a part of the GRIPS intercomparison project for SPARC, and supported in part by the Grant-in-Aid for Scientific Research of the Japanese Ministry of Education, Culture, Sports, Science and Technology. The study with the Berlin GCM has been funded by the European Commission under the contract No. EVKZ-CT-1999-00001 (SOLICE). The FUB GCM simulations were performed at the Konrad-Zuse-Zentrum für Informationstechnik, Berlin.

References

Haigh, J. D., The role of stratospheric ozone in modulating the solar radiative forcing of climate, *Nature*, *370*, 544–546, 1994.

Haigh, J. D., A GCM study of climate change in response to the 11-year solar cycle, *Q. J. R. Meteorol. Soc.*, *125*, 871–892, 1999.

Hood, L. L., J. L. Jirikowic, and J. P. McCormack, Quasi-decadal variability of the stratosphere: Influence of long-term solar ultra violet variations, *J. Atmos. Sci.*, *50*, 3941–3958, 1993.

Huang, T. Y. W., and G. P. Brasseur, Effect of long-term solar variability in two-dimensional interactive model of the middle atmosphere, *J. Geophys. Res.*, *98*, 20,413–20,427, 1993.

Kodera, K., On the origin and nature of the interannual variability of the winter stratospheric circulation in the Northern Hemisphere, *J. Geophys. Res.*, *100*, 14,077–14,087, 1995.

Kodera, K., and Y. Kuroda, Dynamical response to the solar cycle, *J. Geophys. Res.*, *107*(D24), 4749, doi:10.1029/2002JD002224, 2002.

Kodera, K., and K. Yamazaki, Long-term variation of upper stratospheric circulation in the Northern Hemisphere in December, *J. Meteorol. Soc. Jpn.*, *68*, 101–105, 1990.

Kuroda, Y., and K. Kodera, Effect of the solar cycle on the Polar-night jet oscillation, *J. Meteolrol. Soc. Jpn.*, *80*, 973–984, 2002.

Langematz, U., and S. Pawson, The Berlin troposphere-stratosphere-mesosphere GCM: Climatology and annual cycle, *Q. J. R. Meteorol. Soc.*, *123*, 1075–1096, 1997.

Lean, J. L., G. J. Rottman, H. L. Kyle, T. N. Woods, J. R. Hickey, and L. C. Pugga, Detection and parameterization of variations in solar mid-and-near-ultraviolet radiation (200–400 nm), *J. Geophys. Res.*, *102*, 29,939–29,956, 1997.

Palmer, T. N., A nonlinear dynamical perspective on climate change, *Weather*, *48*, 314–326, 1993.

Pawson, S., et al., The GCM-reality intercomparison project for SPARC (GRIPS): Scientific issues and initial results, *Bull. Am. Meteorol. Soc.*, *81*, 781–796, 2000.

Randel, W. J., Global atmospheric circulation statistics, 1000–1 mb, *NCAR Tech. Note NCAR/TN-366+STR*, 256 pp., Natl. Cent. for Atmos. Res., Boulder, Colo., 1992.

Shibata, K., H. Yoshimura, M. Ohizumi, M. Hosaka, and M. Sugi, A simulation of troposphere, stratosphere and mesosphere with an MRI/JMA98 GCM., *Pap. Meteorol. Geophys.*, *50*, 15–53, 1999.

Shindell, D. T., G. A. Schmidt, R. L. Miller, and D. Rind, Northern Hemisphere winter climate response to greenhouse gas, ozone, solar, and volcanic forcing, *J. Geophys. Res.*, *106*, 7193–7210, 2001.

K. Kodera, Y. Kuroda, and K. Shibata, Meteorological Research Institute, 1-1, Nagamine, Tsukuba, Ibaraki 305-0052, Japan. (kodera@mri-jma.go.jp; kuroda@mri-jma.go.jp; shibata@mri-jma.go.jp)

U. Langematz and K. Matthes, Institut für Meteorologie, Freie Universität Berlin, Carl-Heinrich-Becker-Weg 6-10, 12165 Berlin, Germany. (matthes@strat01.met.fu-berlin.de; lang@strat01.met.fu-berlin.de)